Mine Water and the Environment (2021) 40:639–656
https://doi.org/10.1007/s10230-021-00771-5

TECHNICAL ARTICLE

Predicted Post-Closure Aqueous Geochemistry at the Cortez Hills Underground Mine, Nevada, USA

Andy Davis[1] · Maggy Lengke[1] · Jerritt Collord[1] · Nathan Sims[1]

Received: 24 January 2020 / Accepted: 22 February 2021 / Published online: 31 August 2021

Abstract

An investigation was undertaken to predict the post-closure water chemistry of the Cortez Hills Underground Deep South Extension where the mine workings will be backfilled with cemented waste rock. The objective was to determine the potential effects of the tunnel water on adjacent groundwater once the groundwater table recovers, hydraulic conditions stabilize, and ambient groundwater flow is reestablished. The average background groundwater chemistry from three wells representing discharge to the tunnel area during closure, and the worst-case groundwater dissolution chemistry of tunnel floor/unconsolidated backfill, shotcrete (sprayed concrete), cemented backfill and country wallrock/cemented backfill reactions were used to calculate their contribution to the total mass loading during tunnel flooding. The volume of groundwater flow through the tunnel area was coupled with these releases to calculate a total tunnel water quality. All analytes met NV Division of Environmental Protection Profile I standards, except for As, Sb, and Pb, due to their naturally-elevated background groundwater levels (0.08, 0.014, and 0.03 mg/L, respectively). The PHREEQC geochemical code was used to determine the post-closure dissolved phase solutes that could migrate to adjacent groundwater. The dissolved tunnel water chemistry was predicted to be pH = 8.2, with an alkalinity of 124 mg/L $CaCO_3$ and with all solutes meeting Profile I except for As (0.07 mg/L) and Sb (0.01 mg/L). The predicted water chemistry was dominated by the influent groundwater, which comprised ≈97% of the mass loading and was similar to two existing underground seeps.

Keywords Cemented backfill · Closure tunnel chemistry · Geochemical modeling · Groundwater · Underground seeps

Introduction

Underground mining typically requires dewatering of the host rock to allow recovery of the resource. Post-closure groundwater will usually recover to ambient conditions when the pumps are turned off, flooding the workings. If the declines and workings were below the pre-mining water level, there is the potential for adverse environmental consequences as the rising groundwater dissolves contaminants left from the exposure of the rock to the atmosphere during mining, and then reaches the ground surface. In contrast, in some deeper mines, the contaminated groundwater may remain below the ground surface, but may contaminate underground aquifers. For example, in Great Britain, there are 19 poor-status groundwater bodies, predominantly due to metal mining, primarily in southwest England, western Wales, and Northumbria (Environment Agency 2008).

In some mines, underground cemented backfill has been used to provide ground support and regional stability, allowing the safe stoping of ore from beneath solidified cemented backfill. The recipe may include fly ash, waste rock, slag, or tailings, with cement added to ensure stability and strength (Kesimal et al. 2004). Despite a dearth of information on the effects of cemented backfill on the environment, it has generally been perceived as positive due to the reduction in the surface footprint of a mine, the mitigation of sulfide reactivity (by the alkaline cement), and the preferential flow of groundwater around the cement (MEND 2006). Questions remain, principally the potential for groundwater to be contaminated by the backfill.

As part of permitting mines on federal lands, the National Environmental Policy Act (NEPA) requires prediction of reasonably-foreseeable impacts to surface and groundwater resulting from new mines. In addition, the Nevada Division of Environmental Protection (NDEP 2020) requires

✉ Andy Davis
andy@geomega.com

[1] Geomega, 2585 Central Ave, Boulder, CO 80301, USA

that underground mines "*avoid the potential degradation of waters of the State by taking or not taking a certain action or parts of an action.*" Consequently, it was necessary to understand the potential effects of these workings on adjacent groundwater.

There has been substantial investigation into the geochemistry of non-paste-backfilled underground workings. For example, Tomiyama et al. (2019) described the geochemistry of groundwater and its flow system in the closed Yatani mine in southern Yamagata Prefecture, Japan, which generates AMD. The study elucidated AMD formation and its flow patterns using geological, hydrological, geochemical, and isotopic techniques. Nordstrom (2017) reported on the presence of a white aluminous precipitate approximating basaluminite at a caved-in mine portal in Colorado, while Newman et al. (2019) investigated the metalliferous sulfate salts from underground mine complexes in Nevada, USA. They found Al-bearing salts to be the most common minerals but urged caution modeling their formation due to the disparity between thermodynamic databases in different models. Roessler et al. (2007) analyzed groundwater in the flooded West Camp underground mine workings, which had a circumneutral pH and contained at least 8 mM aqueous sulfide with elevated Mn (90 mM), Fe (16 mM), and As (1.3 mM). Dissolved inorganic carbon was in chemical and isotopic equilibrium with rhodochrosite in the mineralized veins, while the mine water was supersaturated with Cu- and Zn-sulfides.

A simple model developed by Younger (2016) for post-closure coal mine water recovery focused on delineation of the master seam and used summary information such as the collar elevations of unfilled shafts, the extent of workings, dewatering pumping rates, and the geometry of any overlying aquifers. While acknowledging the importance of post-mining tunnel chemistry in a coal mine, it was felt that accurate prediction of a wide range of parameters were beyond curent capabilities (Younger and Robbins 2002) with only a simplified prediction protocol available for total iron (Younger 2000, 2016).

Nevertheless, predicting future water quality at hardrock mine sites has been practiced for at least the past 30 years (Maest et al. 2005). For example, the MINEWALL (MEND 1995) approach and code provides a method to predict water quality in open submerged workings. However, the effect of cemented backfill on the eventual quality of groundwater adjacent to the workings after reconstitution of post-closure ambient groundwater flow conditions has apparently not been considered, despite the obvious potential benefits of the cement's alkalinity. This paper explores a novel approach to evaluate such circumstances using generally accepted analytical methods to evaluate leaching of the country rock to represent the open tunnel perimeters and uncemented waste rock, solute diffusion from shotcrete (sprayed concrete) and cemented rock, and water/rock reactions at the cement/backfill wall rock interface as groundwater recovers through the workings. The objective was to determine if the tunnel water would adversely affect the adjacent groundwater once hydraulic conditions stabilize and ambient groundwater flow is reestablished.

Mine Setting

The Cortez Hills underground (CHUG) mine in southern Crescent Valley, Nevada (Fig. 1) is located within the Basin and Range physiographic province where the assemblage comprises complex faulted and folded Paleozoic sedimentary strata with widespread occurrences of Jurassic, Cretaceous, and Tertiary intrusive and volcanic rocks. The Cortez Hills deposit is hosted primarily in the Devonian Wenban (DW) and Silurian Roberts Mountains (SRM) limestones, which consist of dark grey, carbon-rich, calcareous to dolomitic siltstones that have been locally altered. The tunnel floor and uncemented backfill lithology (Fig. 2) is composed of the SRM, intrusives (INT), consisting of quartz monzonite, quartz porphyry dikes, and tuff; Ordovician Hanson Creek (OHC), primarily a mudstone unit, and DW formations (Table 1). The existing open pit mine will eventually be ≈ 630 m deep with a surface exposure of ≈ 400 ha. There will be no AMD from the Cortez Hill open pit above the CHUG because the pit is hosted predominantly in limestone and although it will be partially backfilled with a combination of 50% Devonian Wenban limestone and 50% alluvium after mining ends, the pit lake will not form until after inundation of the workings and is predicted to have a circumneutral pH with water chemistry that meets Profile III (BLM 2018).

The CHUG mine is immediately below the base of the Cortez Hills pit and will eventually reach a depth of ≈760 m above mean sea level (amsl) by the end of 2032. The CHUG's declines are accessed through portals on the wall of an old open pit and are mined primarily by underhand cut-and-fill methods with a portion of the waste rock replaced as cemented backfill in mined-out portions of the underground workings. The CHUG access workings (≈570,000 m^3), with their shotcreted ribs and roof with a rock floor, will constitute void space available for groundwater inundation (Fig. 3). All other workings (≈2.26 million m^3 below 1160 m amsl) will be stoped and backfilled with either consolidated rock or cemented backfill (Fig. 4).

The ultimate dewatering level (≈760 m) will be ≈720 m below the pre-mining water level in the mine area. Based on the groundwater model (SRK 2017), CHUG groundwater levels will recover to within 3 m (1,477 m amsl) of the pre-mining water levels (1,480 m amsl) within ≈30 years of the end of mine life, currently scheduled for 2032. The model predicts a rapid (≈30 m/year) rate of water level recovery

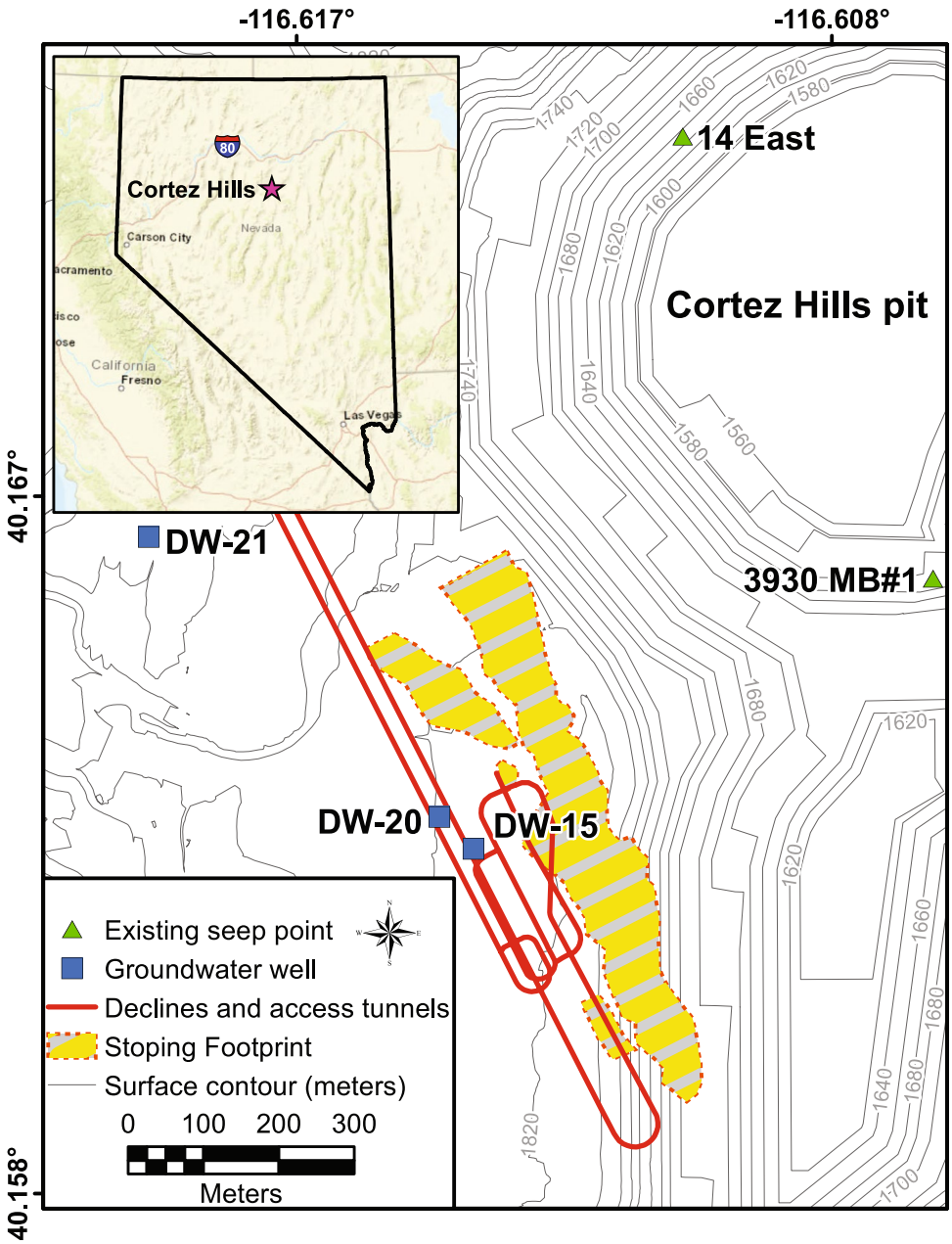

Fig. 1 Location of the Cortez Hills Underground Mine tunnels under the Cortez Hills pit. The existing seeps are in access tunnels above the main workings

after dewatering ceases, inundating the CHUG workings in < 5 years (see Supplemental Material on the groundwater model).

As workings are rapidly inundated, oxidation reactions will virtually stop because O_2 diffusion in water is three orders of magnitude less than in air (Davis and Ritchie 1986), greatly reducing the oxidation rates of pyrite following submersion. Therefore, the loading from the different compartments (commonly referred to as the first flush (Gzyl and Banks 2007) were simulated by short-term release of solutes from leaching tests. As anticipated, most tests released the highest solute concentrations at week 0 (supplemental Tables S1 through S6); however, if higher concentrations appeared in later weeks, these were used in an abundance of caution.

Solute mass in the workings will emanate from: groundwater entering the coarse backfill in the tunnel when the pumps are turned off; dissolution of tunnel floor and unconsolidated waste rock, shotcrete, and; cemented backfill/tunnel wall interactions. The cumulative mass loading from these sources was integrated to derive the total tunnel chemistry. The tunnel geochemical post-closure model was constructed based on the tunnel geology, acid–base accounting (ABA), humidity cell tests (HCTs), cemented backfill and shotcrete dissolution tests, column tests, and groundwater chemistry using procedures explained below.

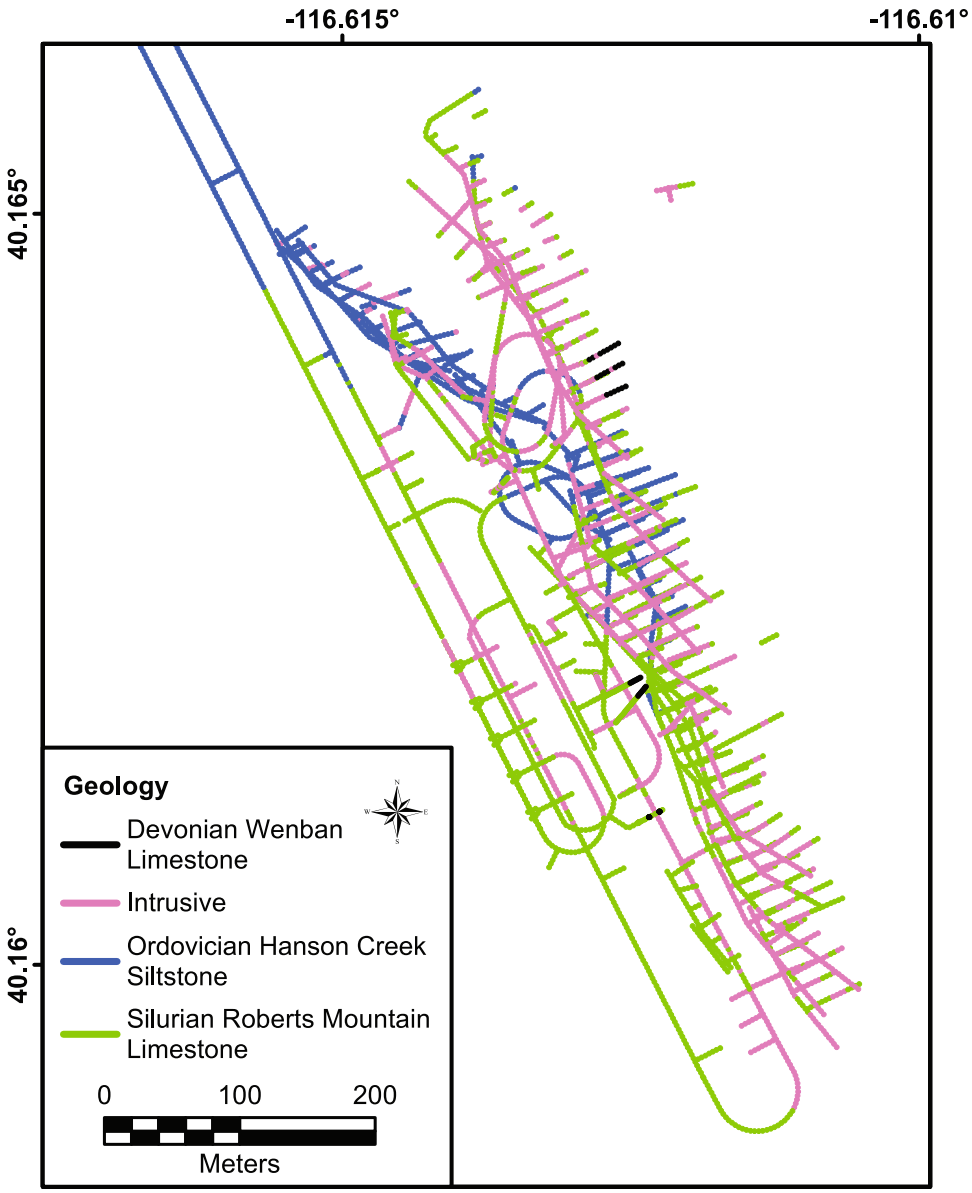

Fig. 2 The geology of the Cortez Hills Underground Mine workings

Table 1 Estimated surface area and percentages of the CHUG Mine tunnel geologic/geochemical model class (945–1,158 m amsl)

Formation	Geochemical model class	Floor surface area		Unconsolidated rock surface area		Cemented wall surface area		Shotcrete wall surface area	
		(m^2)	(%)	(m^2)	(%)	(m^2)	(%)	(m^2)	(%)
Silurian roberts mountains	SRM Code 1	38,074	33.8						
	SRM Code 2	8,267	7.3						
Intrusive	INT Code 1	26,787	23.8						
	INT Code 2	8,384	7.5						
	INT Code 3	3,304	2.9						
Devonian Wenban	DW Code 1	2,200	2.0						
Ordovician Hanson Creek	OHC Code 1	25,495	22.7						
Unknown	Unknown			1,52,547	100	13,424	100	3,27,297	100
Total		**1,12,510**	**100**	**1,52,547**	**100**	**13,424**	**100**	**3,27,297**	**100**

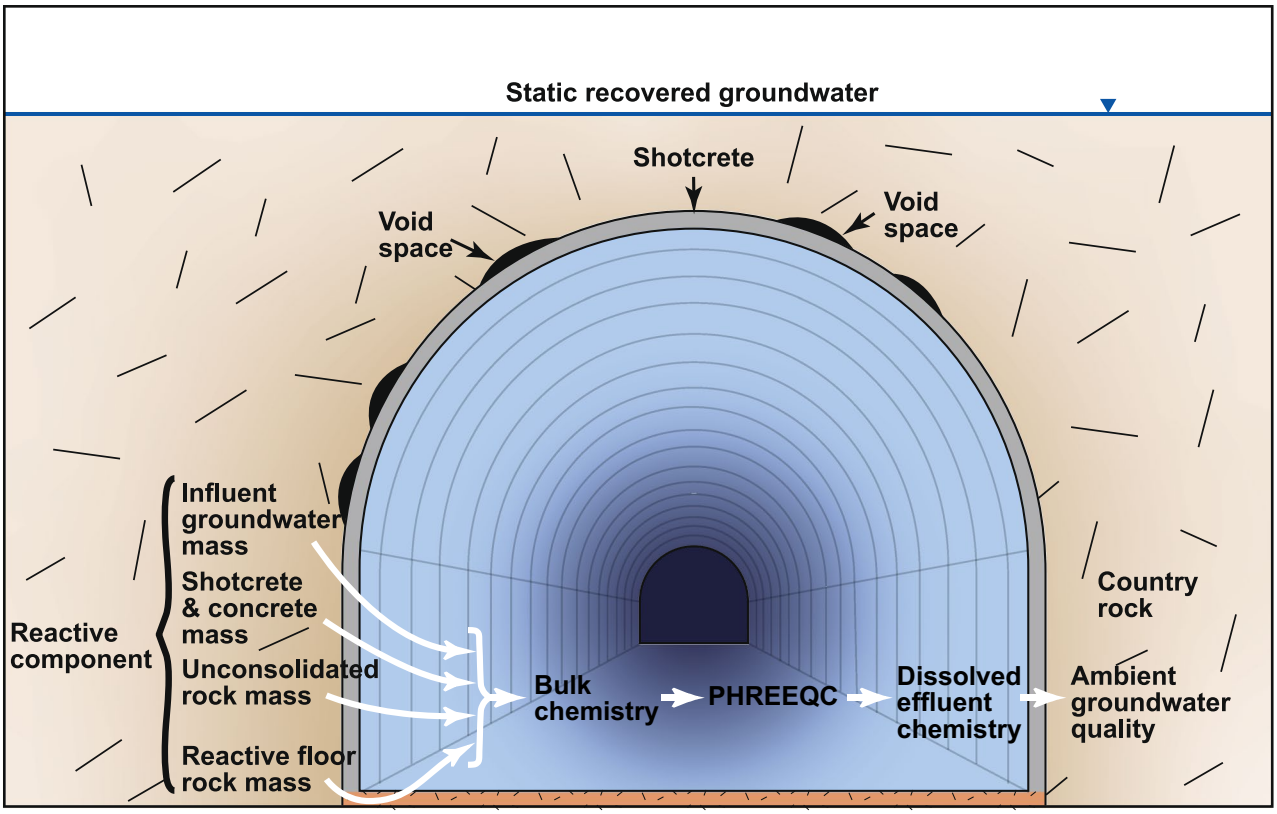

Fig. 3 Conceptual model of solute mass discharge and reactions in the tunnel area after closure and inundation of the underground workings

Materials and Methods

Working Volume Estimates

A three-dimensional (3D) geologic model (included as Supplemental Material) was built with Leapfrog© geologic software using surfaces and drilling contacts to identify the lithologies that intersect the tunnels, and then to select representative rock for material characterization.

Computer-aided design (CAD) drawings of the primary access workings (i.e., Range Front declines and associated secondary access drifts, ramps, vents, and ore pass raises on the southwest side of the ore deposit) and a block model with an estimated ore cutoff in the oxidized lower zone ore were used to define the material to be removed, and hence the extent of the underground workings. The stoped volumes were estimated assuming 38.4 m thick units from the 1158 m level down to the 760 m elevation. A network of tertiary access drifts totaling 10,363 m was generated from the major "arterial" transportation routes (7315 m) below the 1158 m elevation and the nearby stopes. The nominal cross section of access drifts was set as 5.5 m wide by 5 m high, with ≈90% (by linear m) of the sub-1,158 m workings having these dimensions, while the remainder were assumed to be 6 m wide by 5 m high, and 8 m wide by 7.6 m high in material transfer areas, with 3.7 m diameter raises. Extraction of ore will occur by long hole stoping in 6 m wide primary stopes, which will be backfilled with cemented rock, alternating laterally with 9 m wide secondary stopes backfilled with unconsolidated rock.

Lateral drifts above and below the stopes occur on 13 m vertical intervals and can be made in either ore or waste as necessary (Fig. 4). The general mining order is from bottom-to-top of the deposit, so that lateral drifts may be used to drill blast holes down through a stope below (if ore exists there), then used for access to backfill the resulting slot raises sequentially. Then, while drilling is occurring 13 m above it, the drift may be used for access to muck the ore from slot raises through the stope volume above it. Lateral access drifts from secondary haulage to the stopes are anticipated to occur in the primary stope areas, so the surface area of the exposed rock was calculated using the product of the number of lateral stope access headings (2281) and their cross-sectional area (5.5 m wide and 5 m high).

The mine site ABA-based geostatistical model for the acid-neutralizing potential (ANP) and acid-generating potential (AGP) was used to geochemically characterize the underground workings in conjunction with the geologic

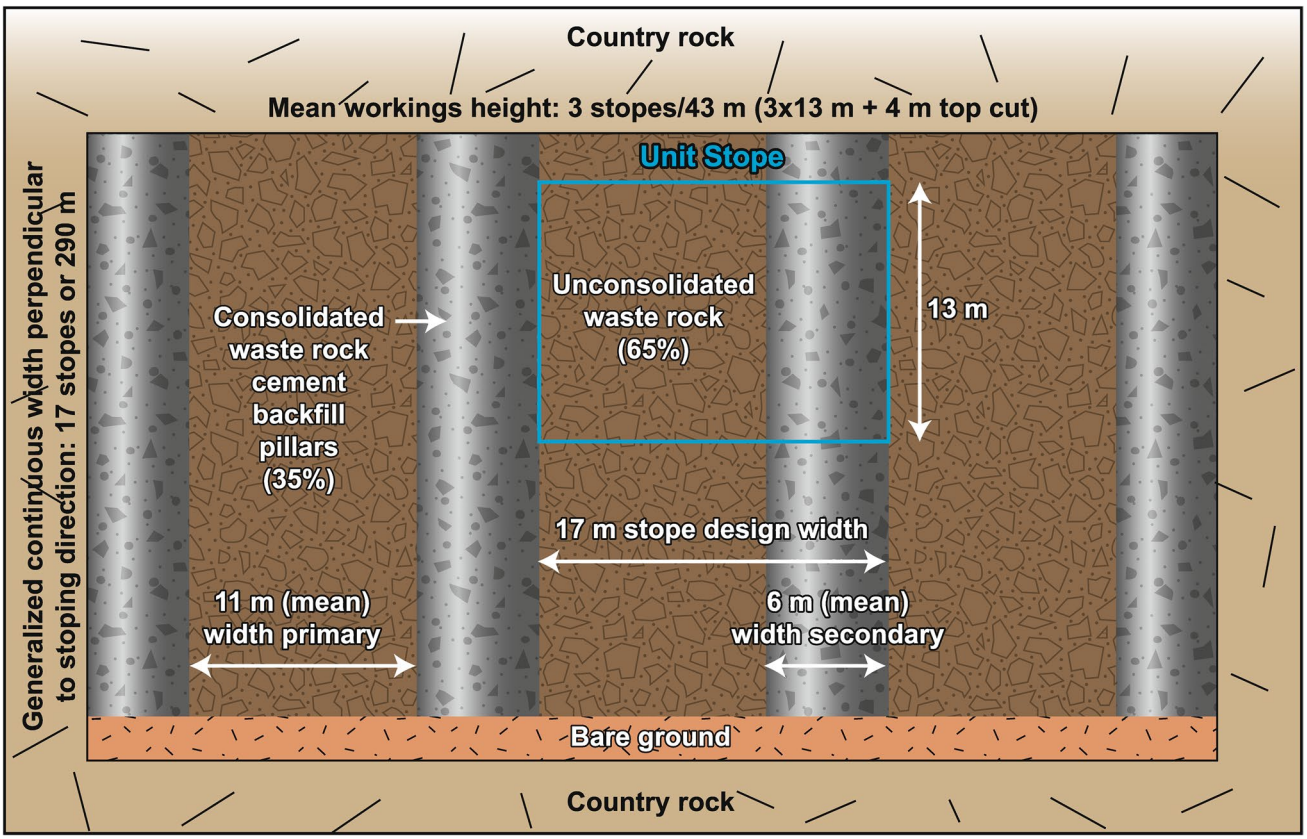

Fig. 4 Cross-section schematic through a typical backfilled stope showing columns andunconsolidated waste rock

model. Full documentation of the geostatistical treatment of samples selected for static and kinetic testing is beyond the scope of this paper. Briefly, the ANP proxy model was based on Ca and Mg because there is dolomite present at the site, while the AGP proxy model was based on total S. Kriging domains were designed to delineate intrusive material from sedimentary material, and variography within each domain was modeled separately. All input data was Z-transformed.

The mine collected ABA data (only total S) but lacked ANP data before introduction of the Nevada modified Sobek method (NVMS), the NDEP-accepted ABA method at the time of this work (NDEP 2015). However, the NVMS is not a cost-effective and practical approach to characterize an entire mining project. In contrast, whole rock inductively coupled plasma (ICP) and total S data are analyzed on nearly every meter of drilling on site and were used to develop the proxy ANP and AGP models that was then compared with the equivalent NVMS data to test the rigor of the proxy model. The correlation between the net-neutralizing potential (NNP = ANP-AGP) proxy model and the NVMS analytical method (Fig. 5a) was robust ($r = 0.98$). Specificity, as defined by the ratio of 48 correct predictions of non-potentially acid-generating (non-PAG) by ICP to the total number (50) of non-PAG samples identified by NSMP results in a predictive accuracy of 96%. In addition, the NNP analyzed using total S and C values obtained by a LECO combustion analyzer (ASTM 2013a, b, c) was an excellent proxy ($r = 0.99$) for the NVMS method (Fig. 5b).

The floor areas of the workings were calculated by tracking the width of the access workings (subsequently called tunnels), discretized into 3 m linear segments for which the HCT chemistry was used to characterize the first flush. Similarly, the surface area of shotcrete in the roof and ribs of the open tunnels was accounted for by the non-floor area in these segments, using the requisite tunnel dimensions and the shotcrete leachate chemistry for this model compartment. The volume of uncemented backfill (≈60%) was estimated from a generalized 15 m wide stope volume that met the cutoff grade and characterized by the HCT chemistry. The cemented backfill, estimated to be 40% of the total backfill volume, was represented by the diffusion test results.

Groundwater and Seep Chemistry

The background groundwater chemistry contribution was based on the well chemistry adjacent to the mine, the volume of water flowing through the tunnel wall rocks obtained from Leapfrog© to determine the configuration and elevation of

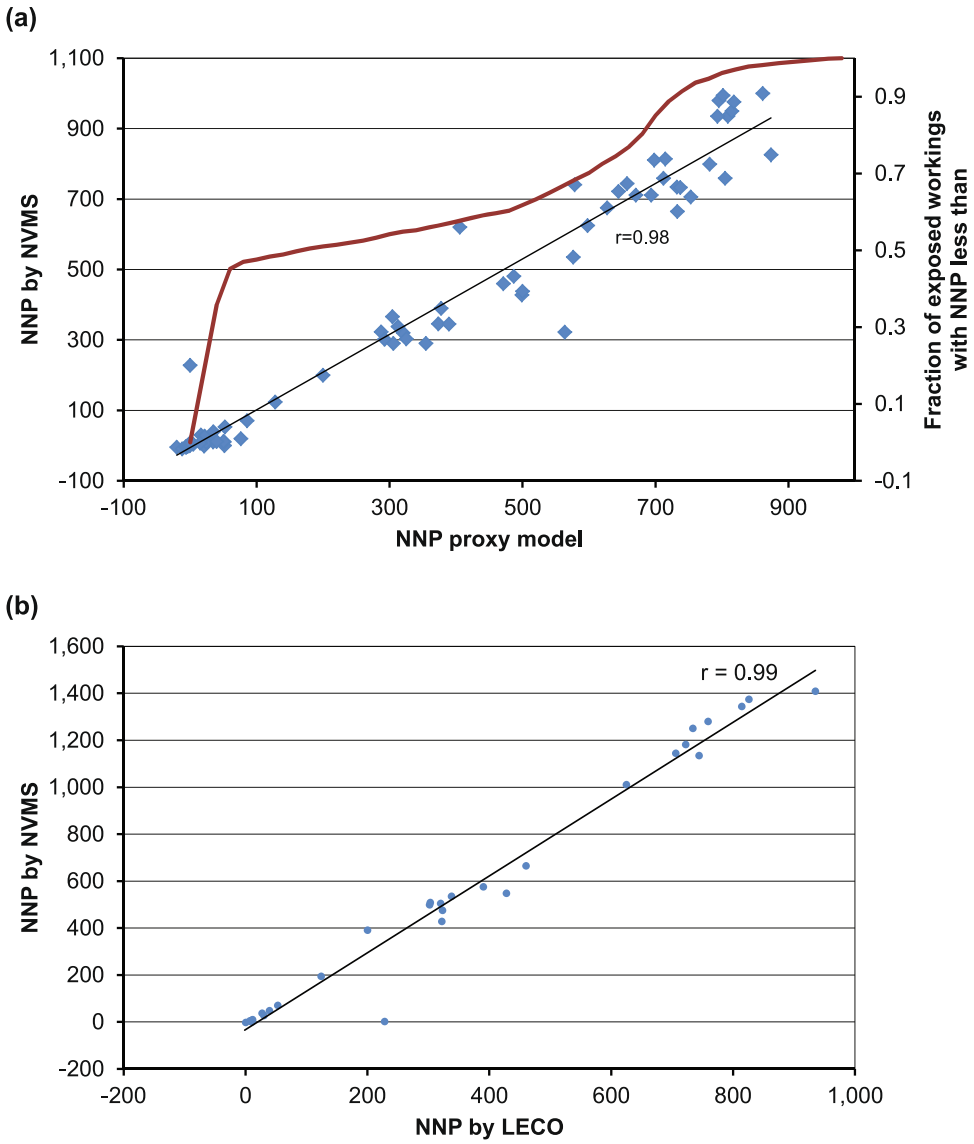

Fig. 5 (**a**) Correlation between the NNP ICP proxy model and the anatytical NVMS method also showing the cummulative NNP frequency distribution, and (**b**) the correlation for NNP between the NVMS and Leco analytical methods

the workings, and the site groundwater flow model (SRK 2017) to determine the recovered, post-closure groundwater elevation (see the Supplemental Material for additional information on the groundwater model).

After dewatering ends, the underground workings will be inundated with groundwater. An average (based on data from 2009 to 2015) of the groundwater chemistry from three wells (DW-15, DW-20, and DW-21), near the tunnel area (Fig. 1) was used to define the background groundwater chemistry used in the model. In addition, two underground samples (14 East and 3930 Muck Bay #1) were collected from pools adjacent to the seeps at higher levels (above 1270 m amsl) in the mine (Fig. 1) and analyzed for NDEP Profile II parameters plus U and total suspended solids (TSS).

Tunnel Floor and Unconsolidated Waste Rock

Humidity cell tests (HCTs) are designed to model the geological processes of weathering at the laboratory scale and were run to comply with the NDEP requirements for materials characterization. Each cell was charged with 1 kg of minus 6.3 mm material and on day 1 (week 0), leached with 1 L of deionized (DI) water and analyzed at the bench for SO_4, Fe^{2+}/Fe^{3+}, and pH. Subsequently, dry air was passed through the cell for 3 days, followed by 3 days of moist air. On the 7th day, another liter of DI water was passed through the cell and analyzed. This process continued on a weekly basis. The required minimum duration for HCTs is 20 weeks to evaluate waste rock reactivity (ASTM 2013a). Metals and

major ions were typically measured at 0, 1, 2, 4, 8, 12, 16, and 20 weeks, and every 4 weeks thereafter, until, if requiring a longer run time, transitioning to 8-week intervals.

The exploration database whole rock ICP dataset together with ABA analyzed by the NVMS method were used to select representative HCT samples based on the indicator parameters (IPs), e.g., ANP, AGP, Al, As, Sb, F, Fe, Hg, Mn, Tl, Se, and SO_4 concentrations cumulative frequency distribution (Davis et al. 2019). From this candidate data set, 11 samples were selected to be run in HCTs that represented the range of chemistry and lithologies distributed throughout the mine (Fig. 6). For metals, the samples cover the lower to the upper case (e.g. the 80th–90th percentiles for As and Fe). For ABA (NNP) the focus was on the lower percentiles for a conservative representation (Fig. 6).

Shotcrete Dissolution Testing

Shotcrete was provided by the Cortez Mine as 10.2 cm diameter cylindrical forms and cut into 15.2 cm tall cylinders, which were subjected to a modified version of the ASTM method C1308-08 (ASTM 2008). Briefly, a sample was placed on a support in a container filled with groundwater from DW-15 (Table 2) at a ratio of 1 cm^2 surface area of solid sample to 10 cm^3 of water to quantify the equilibrium chemistry. Whereas ASTM C1308-08 requires the entire volume of water in the vessel to be replaced at each sampling interval, the water was not replaced in this study because the focus was to achieve equilibrium between the groundwater and the shotcrete. Consequently, on analytical days (1, 2, 4, 8, 12, 16, 20, 24, 28, and 32), only the volume of water that was collected for sampling was replaced. Also, the water in the reaction vessel was gently circulated to ensure mixing at all times. Samples were analyzed for Profile II and U through day 32.

Cemented Backfill Dissolution Testing

Testing followed the same modified ASTM C1308-08 (ASTM 2008) method using DW-15 groundwater (as for the shotcrete). A 10.2 cm × 15.2 cm cemented backfill form was provided by the Cortez Mine which was prepared using Portland cement. Analytical samples were collected on day 1 and 32 for Profile II, with pH and specific conductivity measured through day 39 to ensure that equilibrium had been achieved. The pH and specific conductivity was measured using a YSI 556 MPS.

Cemented Backfill and Acid-Generating Wall Rock Reactivity Testing

Three saturated column tests were run with mixed acid-generating wall rock and cemented backfill using DW-15 groundwater as the lixiviate to represent the potential impacts to groundwater from contact at the acid-generating rock and cemented backfill interface. The three CHUG rock samples that generated acidity, CHUE-252_594-609, CHUE-282_563-583 and DC-261_2230-2249 (supplemental Table S-1), were each mixed with crushed, cemented backfill at a 1:1 weight ratio. The waste rock and cemented backfill was stage crushed to < 6.35 mm to meet the ASTM D5744-13 criterion (ASTM 2013a). A riffle splitter was used to obtain homogenous splits of each rock and cemented backfill sample before each were blended (ASTM 2013b). An additional split of each end member was analyzed for particle size analysis by ASTM D422-63 (ASTM 2007) to ensure all HCT and cemented backfill samples had a homogeneous particle size distribution, ranging from < 0.075 to 4.75 mm. After each rock sample was mixed with an equal mass of cemented backfill, the combined material was passed through the riffle splitter again to ensure each mixture was well blended before being loaded into the column.

Column testing was designed following ASTM D4874-95 (ASTM 2014) with acid-generating rock and cemented backfill blends loaded into 10.2 cm ID × 30.5 cm PVC columns, and the mass recorded. Each column was capped with a 0.4 kg/m polypropylene felt filter to contain sample fines. DW-15 groundwater was pumped into the columns in upflow mode at a target rate of 1 L/day, corresponding to the average pore volume of all of the columns (≈1 L) and at a rate approximating groundwater flow (Geomega 2008). Leachate was routinely weighed and analyzed for pH, temperature, and specific conductivity before analysis for Profile II parameters according to the testing schedule (i.e., 1, 2, 4, 8, 12, 16, 20, 24, 28, 32, and 44 weeks).

Geochemical Modeling

The solute loading factors were integrated to derive a net tunnel total chemistry and the dissolved chemistry determined from the total applying the PHREEQC (Parkhurst and Appelo 1999) interactive version 3.3.5.10806, in conjunction with the Minteq.v4.dat (Allison et al. 1991) thermodynamic database to the total chemistry. The objective was to determine potential impacts relative to NDEP Profile I reference values (the groundwater protection levels) to the surrounding groundwater once throughflow conditions are reestablished.

PHREEQC is a computer program that simulates aqueous chemical reactions. The program is based on equilibrium chemistry of an aqueous solution interacting with minerals, gases, solid solutions, exchangers, and sorption surfaces (Parkhurst and Appelo 1999). For CHUG, the code was used as a speciation program to calculate saturation indices, the distribution of aqueous species, and to evaluate sorption to amorphous ferric hydroxide (ferrihydrite) based on empirical observation in shallower underground workings (e.g., Fig. 7, Site 3).

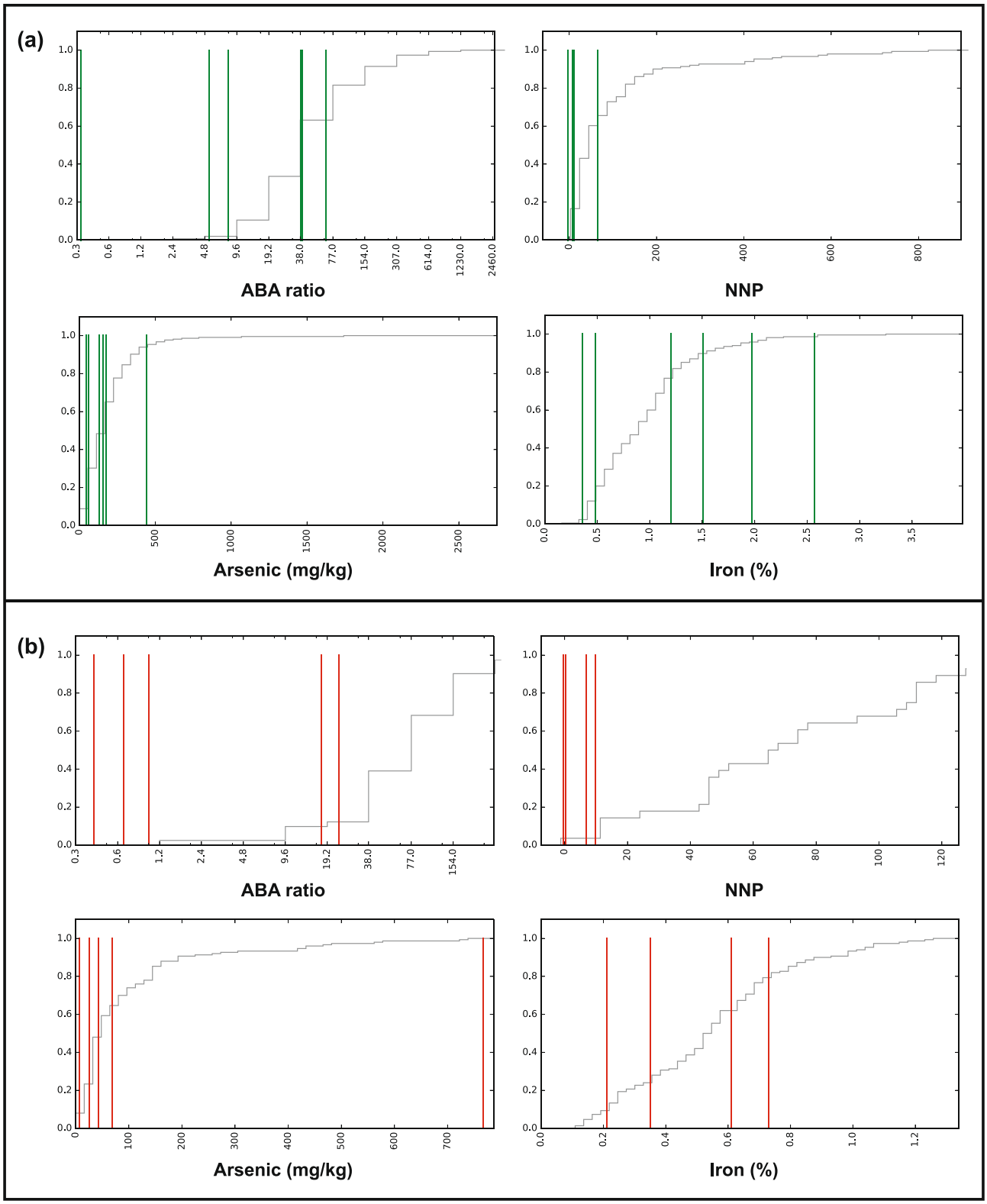

Fig. 6 CHUG HCT samples selected from indicator parameter cumulative frequently distribution for the (**a**) Siluriana Robertsa Mountain and (**b**) Intrusive formation

Table 2 Background groundwater chemistry (mg/L)

Parameters	Profile II	DW-15	DW-20	DW-21	Average
Aluminum	0.2	0.012	0.013	0.023	0.016
Antimony	0.006	**0.01**	**0.006**	**0.03**	**0.014**
Arsenic	0.01	**0.05**	**0.05**	**0.15**	**0.08**
Barium	2	0.10	0.11	0.13	0.11
Beryllium	0.004	0.001	0.001	0.001	0.001
Bicarbonate (HCO_3)	–	224	211	241	225
Bismuth	–	0.005	0.005	0.005	0.005
Boron	–	0.15	0.11	0.20	0.15
Cadmium	0.005	0.001	0.001	0.001	0.001
Calcium	–	39	38	42	40
Chloride	400	18	14	21	18
Chromium	0.1	0.005	0.005	0.005	0.005
Cobalt	–	0.005	0.005	0.005	0.005
Copper	1	0.005	0.005	0.005	0.005
Fluoride	4	0.84	0.54	1.17	0.85
Gallium	–	0.05	0.05	0.05	0.05
Iron	0.6	0.17	0.19	0.40	0.25
Lead	0.015	0.001	0.001	**0.09**	**0.03**
Lithium	–	0.1	0.06	0.15	0.1
Magnesium	150	16	17	17	17
Manganese	0.1	0.014	0.01	0.021	0.015
Mercury	0.002	0.0005	0.0005	0.0005	0.0005
Molybdenum	–	0.02	0.01	0.18	0.07
Nickel	0.1	0.005	0.005	0.005	0.005
NO_2/NO_3 As N	10	0.05	0.05	0.11	0.07
pH	6.5–8.5	8.04	8.39	8.42	8.25
Phosphorus	–	0.05	0.05	0.05	0.05
Potassium	–	7.8	7.1	8.7	7.8
Scandium	–	0.05	0.05	0.05	0.05
Selenium	0.05	0.0025	0.0025	0.0025	0.0025
Silver	0.1	0.005	0.005	0.005	0.005
Sodium	–	39	30	51	40
Strontium	–	0.53	0.40	0.62	0.52
Sulfate	500	46	46	63	52
Thallium	0.002	0.0005	0.0005	0.0005	0.0005
Tin	–	0.016	0.005	0.005	0.009
Titanium	–	0.005	0.005	0.005	0.005
Total Alkalinity ($CaCO_3$)	–	185	178	207	190
Total Dissolved Solids	1,000	312	295	363	323
Vanadium	–	0.005	0.005	0.005	0.005
Zinc	5	0.005	0.005	0.005	0.005

su standard units

Bold font indicates above the NDEP Profile II standards

Equilibrium phases set in the model allowed the tunnel solution to precipitate solids, while solute sorption to ferrihydrite was estimated using the double layer model (DLM) to calculate solute distribution between dissolved and surface (adsorbed) forms using standard parameters of 550 m^2/g for the ferrihydrite surface area, 0.005 high affinity sites per mole, and 0.2 low affinity sites per mole (Dzombak and Morel 1990). The PHREEQC simulation was run at 25 °C, consistent with the basis for the thermodynamic data set.

Two sensitivity analyses were run. The first compared the resulting dissolved solute concentrations for a mineral assemblage consisting of ferrihydrite [$Fe(OH)_3$], gibbsite [$Al(OH)_3$], gypsum ($CaSO_4$), fluorite (CaF_2), barite ($BaSO_4$), calcite ($CaCO_3$), and manganite (MnOOH) with one including only ferrihydrite and calcite, both visually observed to be precipitating in the CHUG workings (Fig. 7). The second evaluated the significance of different thermodynamic data by evaluating the effect of three different ferrihydrite log Ks [3.191 in the Minteq.v4.dat database, 3.0 (Nordstrom 2020), and 4.891 from Minteq.dat] to determine if the precipitating mass had any effect, and whether this affected the attendant sorption of the trace metals As, Cd, Cr, Cu, Hg, Mo, Ni, Pb, Se, Tl, and Zn.

Results

Groundwater and Seep Chemistry

The average groundwater chemistry is an alkaline (190 mg/L $CaCO_3$), pH 8.25 water with a TDS of 323 mg/L and As, Sb, Fe, Pb, and SO_4 of 0.08, 0.014, 0.25, 0.03, and 52 mg/L, respectively (Table 3). Cadmium, Cr, Co, Cu, Hg, Se, and Ag were not detected, so a value equal to half the detection limit was used in the tunnel chemistry model (EPA 1997). All analytes met Profile I, except for As, Sb, and Pb, which are naturally elevated in this region.

The seep water is predominantly a mixed calcium-magnesium bicarbonate type with an alkalinity of 126–148 $CaCO_3$ and TDS of 210–430 mg/L. Arsenic in the 3930 Muck Bay #1 and 14 East locations seeps (0.09 mg/L or 0.02 mg/L, respectively) exceeded Profile I (0.01 mg/L) compared to native groundwater from well DW-15 (0.047 mg/L), with no other constituents above Profile I (Table 3). The highest U (0.006 mg/L) at 3930 Muck Bay #1 was less than the U.S. Environmental Protection Agency (EPA) drinking water maximum contaminant level of 0.03 mg/L.

Tunnel Floor and Unconsolidated Waste Rock

In accordance with Bureau of Land Management (BLM 2013) guidelines, each geologic unit was subdivided into the following categories based on acid base accounting (ABA) data, taking into consideration the ANP, AGP, and NNP, i.e.: Code 1: non-acid-generating (NNP > 20 and ANP/AGP > 3); Code 2: uncertain (0 ≤ NNP ≤ 20 or ANP/AGP ≤ 3), and;

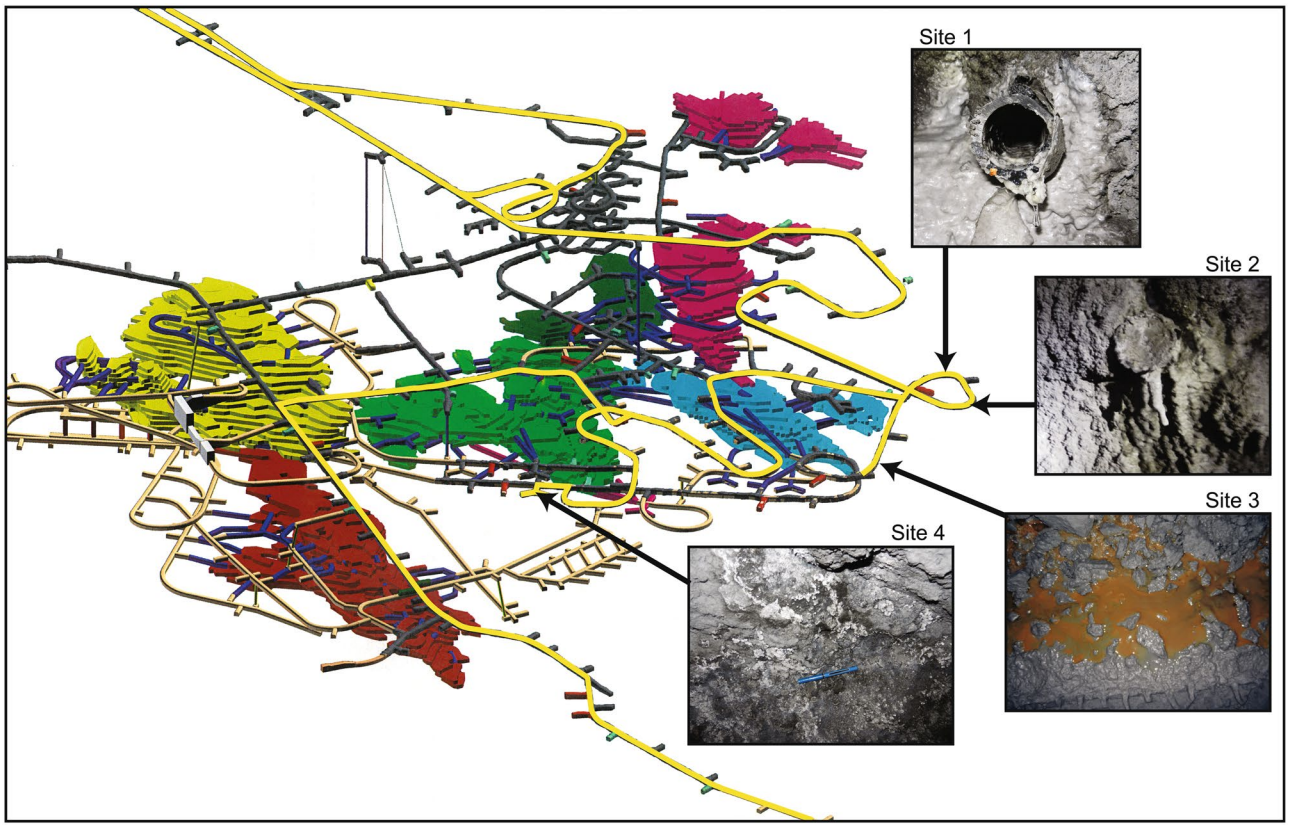

Fig. 7 The Cortez Hills Underground Mine network showing the tunnels traversed during a precipitate investigation (in yellow).The white material at site 1, 2 and 4 effervesced with HCl application indicative of carbonate, while site 3 appeared to be ferrihydrite

Code 3: acid generating (NNP < 0). The tunnel floor area is dominated by Code 1 (non-acid generating) rock, which together constitutes ≈82% of the total CHUG floor area (Table 1; Fig. 8), 15% Code 2 (uncertain) rock and 3% Code 3 (acid-generating).

The different lithologies and geochemical classes along the length of the tunnel floor were represented by 31 HCTs and the 5 SRM Code 2 for the waste rock because the exact constitution is unknown. The ABA of the HCTs (which ran for 20–152 weeks depending on their reactivity) ranged from 0.33–132 and the effluent pH from 3.2–7.9 (Table 3), with leachate exhibiting a wide range of dissolved major, minor, and trace element concentrations (supplemental Table S-1). ASTM (2013a) requires HCTs to be run a minimum of 20 weeks duration; however, they were only terminated when selected indicator leachate parameters became stable.

Shotcrete Dissolution Testing

Over 32 days of shotcrete dissolution, the pH ranged between 8.45–8.9, with the highest pH (8.9) on day 1. Total dissolved solids (TDS) remained less than the influent groundwater concentration for the duration of the test (248–299 mg/L), corresponding with the specific conductivity (supplemental Table S-2). Arsenic (0.04 mg/L) similarly remained less than the influent groundwater.

Cemented Backfill Dissolution Testing

The pH peaked at 10.8 based on the continuous laboratory measurement at day 25 before declining to 10.4 at day 32 (supplemental Table S-3). The highest TDS (427 mg/L) occurred on day 32, corresponding with the highest specific conductivity. Arsenic remained less than the influent groundwater for the duration of the test.

Cemented Backfill and Acid Generating Wall Rock Reactivity Testing

All three saturated columns, containing a 50%:50% ratio of acid-generating rock and cemented backfill, behaved in a similar manner. The porosity of the three columns ranged from 40–43.5%, with all three of the column effluents reaching a maximum pH (≈12.7) on day 1, after one pore volume

Table 3 Cortez Hills Underground Mine HCT and column acid–base accounting results

Sample type	Sample ID	Geology	Total S (%)	Pyrite S (%)	Pyrite S-HCl (%)	Sulfate S (%)	Non-Sulfate S (%)	AGP	ANP	NNP	ABA	Duration	pH	Geochemical Model Class
HCT	CHUE-252_594-609	SRM	0.19	0.15	0.11	0.04	0.15	4.6	1.5	−3.1	0.33	20 wks	4.2	Code 3
	CHUE-282_563-583	SRM	0.08	0.04	0.02	0.04	0.04	1.4	7	5.6	5.0	20 wks	4.2	Code 2
	CHUE-305_785-804	SRM	< 0.01	< 0.01	< 0.01	< 0.01	< 0.01	< 0.3	11.5	> 11.2	76.7	20 wks	7.2	Code 2
	CHUE-322_158-179.5	SRM	< 0.01	< 0.01	< 0.01	< 0.01	< 0.01	< 0.3	12	> 11.7	80	20 wks	7.4	Code 2
	DC-224 2450–2460	SRM	< 0.01	< 0.01	< 0.01	< 0.01	< 0.01	< 0.3	2.4	> 2.1	16	112 wks	5.8	Code 2
	DC-259 2720–2730	SRM	< 0.01	< 0.01	< 0.01	< 0.01	< 0.01	< 0.3	19.8	> 19.5	132	112 wks	6.1	Code 2
	CH07-013-D1_3127.5–3147	SRM	< 0.01	< 0.01	< 0.01	< 0.01	< 0.01	< 0.3	675	675	2250	48 wks	7.5	Code 1
	CHUE-231_507-517	SRM	0.09	< 0.01	0.07	0.09	< 0.01	< 0.3	428	428	1427	48 wks	7.6	Code 1
	CHUE-310_508-523	SRM	0.42	0.2	0.24	0.21	0.2	6.4	833	826	130	48 wks	8.3	Code 1
	CHUE-359_1013-1023	SRM	0.24	0.07	0.24	0.17	0.07	2.3	735	733	320	48 wks	8.1	Code 1
	DC-264 2070–2080	SRM	0.45	0.19	0.34	0.26	0.19	5.9	444	438	75	68 wks	7.5	Code 1
	DC-264 2130–2140	SRM	0.11	< 0.01	0.1	0.11	< 0.01	< 0.3	345	345	1150	68 wks	7.5	Code 1
	DC-261_2230-2249	INT	0.06	0.05	0.05	0.02	0.05	1.5	1	−0.5	0.67	20 wks	4.3	Code 3
	DC-261 2420–2430	INT	0.62	0.5	0.44	0.13	0.5	15.5	6.3	−9.2	0.41	152 wks	3.2	Code 3
	DC-224_2740-2760	INT	< 0.01	< 0.01	< 0.01	< 0.01	< 0.01	< 0.3	< 0.3	> 11.2	1	20 wks	6.8	Code 2
	DC-205_2380-2397	INT	< 0.01	< 0.01	< 0.01	< 0.01	< 0.01	< 0.3	7	> 6.3	46.7	20 wks	7.1	Code 2
	DC-218_2256-2274	INT	0.03	0.02	0.02	< 0.01	0.02	0.6	10.5	9.9	17.5	20 wks	7.3	Code 2
	CHUE-231_317-332	INT	< 0.01	< 0.01	< 0.01	< 0.01	< 0.01	< 0.3	27	27	90.0	48 wks	7.7	Code 1
	DC-272_2375-2385	INT	0.04	0.02	< 0.01	0.01	0.02	0.7	21.5	20.8	30.7	58 wks	7.6	Code 1
	DC-174_1930-1940	INT	< 0.01	< 0.01	< 0.01	< 0.01	< 0.01	< 0.3	25.1	25.1	83.7	104 wks	7.4	Code 1
	DC-189_2150-2160	INT	0.12	0.12	0.11	< 0.01	0.12	3.7	110	106	29.7	68 wks	7.4	Code 1
	CHUE-359_1211-1223	OHC	0.05	< 0.01	0.04	0.05	< 0.01	< 0.3	980	980	3266.7	20 wks	7.2	Code 1
	DC-200_2420-2440	OHC	0.56	0.37	0.42	0.19	0.37	11.5	823	811	71.6	20 wks	7.3	Code 1
	DC-261_2597-2607	OHC	3.08	0.43	1.91	2.65	0.43	13.6	758	744	55.7	20 wks	7.4	Code 1
	DC-263_2170-2180	OHC	0.05	< 0.01	0.04	0.05	< 0.01	< 0.3	460	460	1533.3	20 wks	7.5	Code 1
	DC-263_2190-2200	OHC	0.1	< 0.01	0.09	0.1	< 0.01	< 0.3	390	390	1300.0	20 wks	7.63	Code 1
	DC-199_2650-2660	OHC	0.32	0.04	0.25	0.29	0.04	1.1	533	532	484.7	80 wks	7.3	Code 1
	DC-259_2780-2790	OHC	< 0.01	< 0.01	< 0.01	< 0.01	< 0.01	< 0.3	994	994	3313.3	84 wks	7.3	Code 1
	DC-261_2550-2560	OHC	1.09	0.69	0.74	0.4	0.69	21.5	222	200	10.3	152 wks	7.9	Code 1
	DC-174_1860-1870	DW	0.29	0.25	0.27	0.04	0.25	7.8	799	791	102.4	84 wks	7.4	Code 1
	DC-174_2050-2060	DW	< 0.01	< 0.01	< 0.01	< 0.01	< 0.01	< 0.3	620	620	2066.7	112 wks	7.5	Code 1
	DC-189_2070-2080	DW	0.05	< 0.01	0.05	0.05	< 0.01	< 0.3	528	528	1761.3	84 wks	7.6	Code 1
Column	CHUE-252_594-609 + Concrete (50:50 mix)	SRM	0.16	< 0.01	0.10	0.16	< 0.01	< 0.3	344	> 343.7	344	44 days	11.8	
	CHUE-282_563-583 + Concrete (50:50 mix)	SRM	0.08	< 0.01	0.03	0.08	< 0.01	< 0.3	332	> 331.7	332	44 days	12.0	
	DC-261_2230-2249 + Concrete (50:50 mix)	INT	0.07	< 0.01	0.02	0.07	< 0.01	< 0.3	337	> 336.7	337	44 days	11.9	

AGP, ANP in ($TCaCO_3$/kT)

Non-extractable S(%) < 0.01 for all samples

ABA = ANP/AGP

NNP = ANP-AGP

(Supplemental Tables S-4, S-5, and S-6). Subsequently, the pH slowly declined in each column to ≈12 by day 44 at the terminus of the test, while the TDS was highest for each column on day 1, subsequently declining steadily.

Alkalinity (370–2,240 mg/L $CaCO_3$) was released from all columns. After pore volume 8, As was always less than the influent groundwater, becoming close to or less than Profile I (0.01 mg/L) by day 44, despite influent groundwater being naturally elevated (0.047 mg/L). Total dissolved solids (1,000–2,240 mg/L) were above Profile I (1,000 mg/L) for all initial pore volumes, but decreased to less than this value by day 24. Aluminum exceeded Profile I starting at day 12, except for DC-261_2230-2249, which had elevated Al from day 1. Barium exceeded Profile I (2 mg/L) in CHUE-282_563-583 and DC-261_2230-2249 during the initial pore volumes, while Se and Tl Profile I exceedances only occurred in the first flush from CHUE-252_594-609 and DC-261_2230-2249, respectively. Lead exceeded Profile I from day 1 through 16 at 0.02 to 0.065 mg/L in CHUE-282_563-283. These data demonstrate that the CHUG acid-generating rocks will not dissolve shotcrete or cemented backfill to any significant extent.

Discussion

The relative mass contribution of each component, i.e., groundwater, tunnel floor, unconsolidated waste rock, shotcrete, and cemented backfill and their interactions with acid-generating wall rock was calculated based on the exposure of surface area to groundwater flooding the tunnel system (Table 1), while the groundwater mass was based on the tunnel void space. The laboratory and field data were used to compute the total chemistry from the individual mass loading components. Interactions between various aqueous components in the CHUG tunnels during closure through the processes of mineral precipitation and sorption, will result in a dissolved chemistry that differs from the total chemistry. The total chemistry was run using the equilibrium geochemical code PHREEQC (Parkhurst and Appelo 1999) to calculate the dissolved tunnel chemistry, which is required to determine if surrounding groundwater in the country rock will be affected, assuming throughflow conditions resume (Fig. 3).

Groundwater Chemistry Mass

The average background chemistry from the three wells near the tunnel was used to calculate the groundwater solute mass loading. The volume of water in the tunnel is ≈362,000,000 L. Therefore, the solute mass loading from the groundwater filling the workings is:

$$\begin{aligned} &\textit{Ground water solute mass } (mg) \\ &= \textit{Average groundwater chemistry } \left(\frac{mg}{L}\right) \\ &\times \textit{ Water volume in tunnel } (L) \end{aligned} \tag{1}$$

Tunnel Floor

The tunnel geochemical model classification was used to select the appropriate kinetic HCT data (Supplemental Table S-1) that represent the mass solute release from each lithological category. The ABA of each sample was used to attribute the HCTs to their geochemical divisions (Table 3). As the groundwater enters the tunnel area, it will react with oxidized floor rock, dissolving solutes depending on the reactivity of the floor rock, as defined by the ABA and referenced to the lithology-specific HCTs. Each geochemical model class HCT was selected to represent Codes 1, 2, or 3 (Table 3). If the lithologic types and geochemical class of the tunnel floor were not covered, the intrusive Code 3 HCT was conservatively selected to represent DW and OHC Code 3 materials, since they are in the same geochemical class.

The solute leachability as each area becomes inundated was represented using an average of the worst-case HCT pore flush in term of As, Sb, or SO_4 for each geochemical class (supplemental Table S-1). There are 6.2 pore volumes flushed per week in a HCT, based on a sample weight of 1 kg, added water volume of 1 L, an assumed porosity of 30%, and an assumed bulk density of 2.65 g/cm^3. One flush of HCT leachate chemistry was used in the calculations.

The surface area of each HCT sample used to determine the mass release per unit area was 0.42 m^2/kg, based on a particle analysis of 8 HCTs (Geomega 2015). The total surface area for each geochemical class in the tunnel floor was used to calculate the total mass loading from the tunnel floor rock.

The maximum extent of floor rock reactivity (100%) was conservatively used in the model based on the bedrock porosity (2%), resulting in the solute mass due to reactive floor rock leaching for each geochemical class (Code 1, 2, or 3) from the SRM, INT, DW, and OHC lithologies, i.e.:

$$\begin{aligned} &\textit{Reactive floor rock mass } (mg) \\ &= \textit{One week of HCT concentration } \left(\frac{mg}{L}\right) \\ &\times \frac{1}{\textit{Number of pore volumes per week } (6.2)} \\ &\times \frac{1\ L}{1\ kg} \times \frac{1}{\textit{HCT Surface Area } \left(\frac{m^2}{kg}\right)} \\ &\times \textit{Tunnel surface floor area } \left(m^2\right) \end{aligned} \tag{2}$$

$$\begin{aligned}&\textit{Total floor rock solute mass (mg)}\\&=\sum \textit{Reactive floor rock mass per geochemical class (mg)}\end{aligned} \tag{3}$$

Unconsolidated Waste Rock Mass

Solutes will also be released as groundwater reacts with unconsolidated waste rock. The solute leachability from each newly inundated area was calculated using an average of the worse-case HCT pore flush in terms of As, Sb, or SO_4 for a corresponding match of the geochemical class unit (supplemental Table S-1), resulting in an estimated individual solute mass from reactive unconsolidated waste rock leaching, i.e.:

$$\begin{aligned}&\textit{Unconsolidated waste rock mass (mg)}\\&=\textit{One week of HCT concentration}\left(\frac{mg}{L}\right)\\&\quad\times\frac{1}{\textit{Number of pore volume at Week1(6.2)}}\\&\quad\times\frac{1L}{1kg}\times\frac{1}{\textit{HCT Surface Area}\left(\frac{m^2}{kg}\right)}\\&\quad\times\textit{unconsolidated waste surface area}\left(m^2\right),\ \textit{so}\end{aligned} \tag{4}$$

$$\begin{aligned}&\textit{The total unconsolidated waste rock solute mass (mg)}\\&=\sum\textit{Reactive unconsolidated waste rock for each geochemical class(mg)}\end{aligned} \tag{5}$$

Shotcrete Mass

The shotcrete loading was computed from:

$$\begin{aligned}&\textit{Shotcrete mass (mg)}\\&=\textit{Shotcrete concentration}\left(\frac{mg}{L}\right)\\&\quad\times\frac{1}{\textit{Surface area of shotcrete test}\left(m^2\right)}\\&\quad\times\textit{Tunnel shotcrete surface area}\left(m^2\right)\\&\quad\times\textit{Volume of shotcrete test water (L)}\end{aligned} \tag{6}$$

The mass loading was calculated using the dissolution test results of CHUG shotcrete (supplemental Table S-2). The difference between the worst-case leachate chemistry and influent groundwater was selected to represent the reactive shotcrete dissolution.

Cemented Backfill Mass

As recovering groundwater migrates through the cemented backfill and shotcrete tunnel wall, it will dissolve a portion of the mass. The mass loading was calculated using the dissolution test results of CHUG cemented backfill (supplemental Table S-3). The difference between the worst-case leachate chemistry and influent groundwater was selected to represent the reactive cemented backfill dissolution. The solute mass loading was obtained from:

$$\begin{aligned}&\textit{Cemented backfill mass (mg)}\\&=\textit{Cemented backfill concentration}\left(\frac{mg}{L}\right)\\&\quad\times\frac{1}{\textit{Surfaceareaofconcretetest}\left(m^2\right)}\\&\quad\times\textit{Tunnel concretesurface area}\left(m^2\right)\\&\quad\times\textit{volume of concrete test water (L)}\end{aligned} \tag{7}$$

Total Tunnel Chemistry

The mass of each solute in the groundwater, tunnel floor and waste rock backfill, shotcrete and cemented backfill was summed and divided by the total volume of water in the tunnel at equilibrium after closure to generate the total chemistry of each individual solute, i.e.:

$$\begin{aligned}&\textit{Total chemistry of each solute}\left(\frac{mg}{L}\right)\\&=\frac{\sum\textit{Solute mass (mg)}}{\textit{Volume of water in tunnel (L)}}\end{aligned} \tag{8}$$

The CHUG tunnel total chemistry is predicted to be similar to groundwater, with a slightly lower pH (7.3) and an alkalinity of 191 mg/L $CaCO_3$. Copper, Cr, Ni, and Tl are predicted to be 0.008, 0.006, 0.007, and 0.0006 mg/L, respectively, slightly elevated compared to the background groundwater (Table 4). The specific behavior of these solutes is a function of their concentrations derived from the dissolution of the tunnel floor rock, unconsolidated rock, and cemented backfill/shotcrete leachate. Antimony, As, B, Cd, Fe, and Pb in the total tunnel chemistry are predicted to be similar to the background groundwater. All solutes meet Profile I except for As (0.07 mg/L), Sb (0.01 mg/L), and Pb (0.01 mg/L) which are consistent with

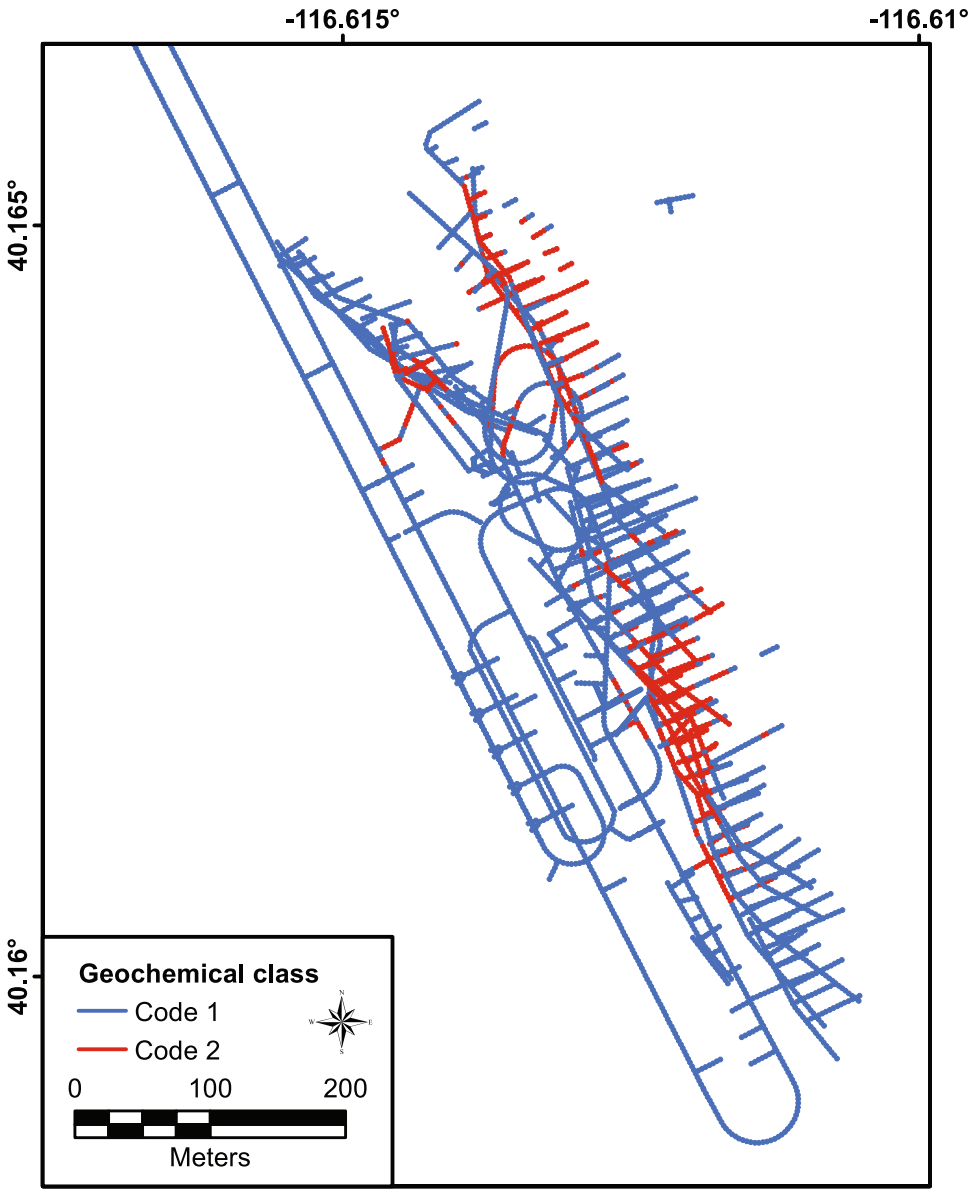

Fig. 8 The geochemical classification (ABA reactivities) of the Cortez Hills Underground Mine workings

area background groundwater chemistry, 0.08, 0.014, and 0.03 mg/L, respectively.

Dissolved Tunnel Chemistry

The dissolved chemistry was computed to evaluate potential effects on the adjacent groundwater as the hydrological regime recovers to pre-mining conditions. Simple equilibrium phases including carbon dioxide (CO_2), oxygen (O_2), ferrihydrite [$Fe(OH)_3$], gibbsite [$Al(OH)_3$], gypsum ($CaSO_4$), fluorite (CaF_2), barite ($BaSO_4$), calcite ($CaCO_3$), and manganite (MnOOH) were allowed to precipitate from the tunnel solution, if geochemically feasible. The value for the partial pressure of oxygen (pO_2) was set to ambient (i.e., $10^{-0.7}$ atmospheres [atm]). Some of these precipitates (i.e., calcite and ferrihydrite) were selected based on their presence in the upper workings of the CHUG mine (Fig. 7).

Atmospheric pCO_2 is $10^{-3.5}$ atm (Langmuir 1997). However, in groundwater, pCO_2 may be substantially higher because CO_2 is produced in the aquifer by microbial degradation of organic matter, precipitation of calcite, and deep biological and thermogenic (e.g. magmatic) sources of CO_2 gas. In the underground workings, groundwater discharging to the tunnel system was precipitating calcite adjacent to its egress as CO_2 degassed (Fig. 7; Sites 1 and 2), i.e.:

$$Ca^{2+} + 2HCO_3^- \leftrightarrow CaCO_3 + H_2O + CO_2 \quad (9)$$

Table 4 Seep Chemistry and the predicted geochemical model sensitivity analysis with precipitating phases and the log K of Ferrihydrite

Parameter	NDEP profile II standard	Predicted total tunnel chemistry	Dissolved tunnel chemistry[1]	Dissolved Tunnel Chemistry[2] Model with Ferrihydrite (log $K = 3.191$)	Dissolved Tunnel Chemistry[2] Model with Ferrihydrite (log $K = 3.000$)	Dissolved Tunnel Chemistry[2] Model with Ferrihydrite (log $K = 4.891$)	Background groundwater chemistry	Average seep chemistry
pH	6.5–8.5	7.98	8.16	8.16	8.16	8.16	8.25	8.3
TDS	1000	349	153	153	153	153	323	320
Total alkalinity ($CaCO_3$)	–	191	124	124	124	124	190	137
Bicarbonate (HCO_3)	–	226	150	150	150	150	225	166
Aluminum	0.2	0.02	0.02	0.02	0.02	0.02	0.02	< 0.02
Antimony	0.006	**0.014**	**0.01**	**0.01**	**0.01**	**0.01**	**0.014**	< 0.003
Arsenic	0.01	**0.08**	**0.07**	**0.07**	**0.07**	**0.07**	**0.08**	**0.06**
Barium	2	0.12	0.06	0.12	0.12	0.12	0.11	< 0.1
Beryllium	0.004	0.001	0.00002	0.00002	0.00002	0.00002	0.001	< 0.002
Boron	–	0.15	0.15	0.15	0.15	0.15	0.15	0.12
Cadmium	0.005	0.001	0.001	0.001	0.001	0.001	0.001	< 0.002
Calcium	–	40	14	14	14	14	40	39
Chloride	400	18.2	18.2	18.2	18.2	18.2	17.9	56
Chromium	0.1	0.006	0.006	0.006	0.006	0.006	0.005	< 0.01
Copper	1	0.008	0.004	0.004	0.004	0.004	0.005	< 0.01
Fluoride	4	0.87	0.87	0.87	0.87	0.87	0.85	0.25
Iron	0.6	0.3	0.00004	0.00004	0.00003	0.0022	0.3	< 0.02
Lead	0.015	**0.03**	0.01	0.01	0.01	0.01	**0.03**	< 0.002
Lithium	–	0.1	0.1	0.1	0.1	0.1	0.1	0.015
Magnesium	150	17	17	17	17	17	17	25.5
Manganese	0.1	0.015	0.0000003	0.02	0.02	0.02	0.015	< 0.01
Mercury	0.002	0.0005	0.0005	0.0005	0.0005	0.0005	0.0005	< 0.001
Molybdenum	–	0.07	0.07	0.07	0.07	0.07	0.07	< 0.01
Nickel	0.1	0.007	0.007	0.007	0.007	0.007	0.005	< 0.01
Nitrate/nitrite as N	10	0.08	0.08	0.08	0.08	0.08	0.07	1.5
Phosphorous	–	0.05	0.05	0.05	0.05	0.05	0.05	< 0.1
Potassium	–	9	9	9	9	9	7.8	9.5
Selenium	0.05	0.003	0.003	0.003	0.003	0.003	0.003	< 0.005
Silver	0.1	0.005	0.005	0.005	0.005	0.005	0.005	< 0.01
Sodium	–	41	41	41	41	41	40	19.5
Strontium	–	0.56	0.56	0.56	0.56	0.56	0.52	0.6
Sulfate	500	52	52	52	52	52	51.6	35.5
Thallium	0.002	0.0006	0.001	0.001	0.001	0.001	0.0005	< 0.001
Tin	–	0.01	0.01	0.01	0.01	0.01	0.009	< 0.01
Uranium								0.0045
Vanadium	–	0.005	0.004	0.004	0.004	0.004	0.005	< 0.01
Zinc	5	0.007	0.006	0.006	0.006	0.006	0.005	< 0.01

All units in mg/L, except for pH in su

Bold font indicates above the NDEP Profile II standards

[1]Ferrihydrite, calcite, gibbsite, gypsum, fluorite, barite, and manganite included in the model

[2]Only ferrihydrite and calcite included in the model

Groundwater equilibrated with carbonate rock has a calculated pCO_2 (from the pH and alkalinity of the Cortez area groundwater) of $10^{-2.7}$–$10^{-3.1}$ atm. Therefore, 10^{-3} was used, assuming that the pCO_2 of the tunnel will be similar that of the adjacent groundwater.

Field data and laboratory experiments have shown that ferrihydrite is the first iron phase to precipitate from solution when Fe^{2+} is oxidized (Langmuir and Whittemore 1971; Schwertmann and Taylor 1977). Ferrihydrite precipitates noted in the CHUG (Fig. 7) will sequester both cations (e.g. Cu^{2+} and Zn^{2+}) and anions (e.g., SeO_4^{3-} and AsO_4^{3-}) from solution by adsorption (Dzombak and Morel 1990; Leckie et al. 1980). The pH was predicted to be 8.2 with an alkalinity of 124 mg/L $CaCO_3$. The dissolved Al, Fe, Mn, and Ba are lower than the total (Table 4) because gibbsite, ferrihydrite, manganite, calcite, and barite (≈0.009, 0.8, 0.03, 65.3, and 0.1 mg, respectively) precipitated from solution. Trace metal adsorption controls the water chemistry due to Fe dissolution from floor and wall rock leachate precipitating as ferrihydrite and sequestering As, Be, Cu, Pb, and Zn, while the total and dissolved tunnel chemistry are similar for B, Cl, Cr, F, K, Mg, Na, N, Se, and SO_4. All solute concentrations meet Profile I with the exception of As (0.07 mg/L) and Sb (0.01 mg/L), which are still slightly less than the background groundwater concentrations (0.08 mg/L and 0.014 mg/L, respectively) due to ferrihydrite sorption.

The sensitivity analysis demonstrated only minor differences in Ba and Mn concentrations using only ferrihydrite and calcite compared to the complete mineral assemblage [Table 4 (columns 5 and 6)] and none for Al, Ca, F, and SO_4 because the respective mineral solubility products were not exceeded. The log K sensitivity analysis demonstrated that the use of different ferrihydrite thermodynamic data did not intrinsically affect either the Fe concentrations or the affiliated trace metal sorption (Table 4; columns 5, 6, and 7).

Comparison to Tunnel Seepage Chemistry

Comparing the model results to the tunnel seep chemistry indicates reasonable agreement between the predicted dissolved post-closure chemistry and the measured seep water chemistry (Table 4). Both the predicted CHUG tunnel and the average seep waters are alkaline (pH 8.2 and 8.3, respectively), with a similar range of As (0.07 mg/L vs. the seep average, 0.056 mg/L), Sb (0.01 mg/L vs. the seep average < 0.003 mg/L), with low concentrations of other trace metals. Sulfate in the predicted CHUG tunnel (56.5 mg/L) is higher than the seep waters (35 mg/L), but consistent with ambient groundwater (52 mg/L). In general, the CHUG tunnel dissolved chemistry prediction appears to be consistent with the combined seep and/or groundwater chemistry. The reason for this is that groundwater contributes the most mass to the total tunnel chemistry (96.7%), followed by the shotcrete (3.1%), cemented backfill (0.2%), and unconsolidated waste rock (0.04%), with 0.004% from the tunnel floor.

Conclusions

Field and laboratory data were coupled with modeling to evaluate the tunnel water chemistry after flooding of the underground workings at the CHUG mine. The objective was to determine if the tunnel water could potentially affect the adjacent groundwater (compared to Profile I) once hydraulic conditions stabilize and ambient groundwater flow is reestablished.

Based on the ABA data (Table 3), it is apparent that the lithology (in this case, a limestone-hosted ore deposit) and a careful comparison of the ANP/AGP and $\%S_{tot}$ should be considered, rather than pure numerical values when assigning risk to AMD potential when the AGP is less than the detection limit. At least in this setting, the mine-obtained total S and C (LECO) data correlated well with the more expensive NVMS method (Fig. 5b) suggesting that if such a demonstration can be made, empirical lab data can provide credible information to the NEPA permitting process.

Allowing precipitates to form in the modeling process is appropriate because the soluble fraction is the potential load to adjacent groundwater. However, even in the absence of precipitates, the water quality resulting from the cemented backfill is good, indicating that the long-term environmental impacts of underground mining using this method will be negligible.

The seep waters collected from the tunnel drainage are a useful analog for the dissolved tunnel chemistry due to the preponderance of the chemical mass being from groundwater ingress. The predicted CHUG dissolved water chemistry was generally in good agreement with the combined seep/groundwater chemistry. Therefore, after inundation of the tunnel system and regeneration of the ambient groundwater flow vectors, any tunnel water migrating into the surrounding country rock is not anticipated to degrade groundwater quality.

Supplementary Information The online version contains supplementary material available at https://doi.org/10.1007/s10230-021-00771-5.

Acknowledgements The authors are grateful to the Cortez mine for the use of their data. While Geomega has had a commercial relationship with the mine, this paper is an independent research effort for which no remuneration was requested. The research did not receive any specific grant from funding agencies in the public, commercial, or not-for-profit sectors. We are grateful for the constructive comments from seven reviewers, which helped to greatly improve the manuscript structure, and for the editorial insights of Anne Weber and Bob Kleinmann.

References

Agency E (2008) Abandoned mines and the water environment (Science project SC030136-41). Bristol

Allison JD, Brown DS, Novo-Gradac KJ (1991) MINTEQA2/PRODEFA2 - A geochemical assessment model for environmental systems (EPA/600/3-91/021). U.S Environmental Protection Agency (EPA)

ASTM (American Society for Testing of Materials) (2007) Standard test method for particle-size analysis of soils (Method D422–63). ASTM International

ASTM (2008) Standard test method for accelerated leach test for diffusive release from solidified waste and a computer program to model diffusive, fractional leaching from cylindrical waste forms (Method C1308–08). ASTM International

ASTM (2013a) Standard test method for laboratory weathering of solid materials using a humidity cell (Method D5744–13). ASTM International

ASTM (2013b) Standard practice for sampling and sample preparation of iron ores and related materials for determination of chemical composition and physical properties (Method E877–13). ASTM International

ASTM (2013c) Standard test method for analysis of metal-bearing ores and related materials for carbon, sulfur and acid-base characteristics (Method E1915–13). ASTM International

ASTM (2014) Standard test method for leaching solid material in a column apparatus (Method D4874–95). ASTM International

BLM (Bureau of Land Management) (2013) Nevada Bureau of Land Management rock characterization and water resources analysis guidance for mining activities. U.S Dept of the Interior

BLM (Nevada Bureau of Land Management) (2018) Final deep south expansion project supplemental environmental report – water resources and geochemistry [Prepared in Support of: File: NVN-067575 (16–1A) DOI-BLM-NV-B010-2016-0052 EIS]. US Dept of the Interior

Davis G, Ritchie A (1986) A model of oxidation in pyritic mine wastes: Part 1, equations and approximate solution. App Math Modeling 10:314–322

Davis A, Whitehead C, Lengke M, Collord J (2019) Acid-base accounting tests in combination with humidity cells help to predict waste rock behavior. Mine Water Environ 38:467–487

Dzombak DA, Morel FMM (1990) Surface complexation modeling: hydrous ferric oxide. John Wiley and Sons

EPA (1997) Non-detect policy (CENAN-OP-SD 28 February 1997). U.S. Environmental Protection Agency (EPA). https://archive.epa.gov/region02/water/dredge/web/html/nondetect.html#:~:text=i)%20If%20a%20concentration%20of,the%20contaminant%20in%20the%20sample. (Accessed 19 Sept 2014)

Geomega (2008) Groundwater quantity and quality assessment of the revised Cortez Hills pit design. Report to Cortez Gold Mines Geomega Inc

Geomega (2015) Cerro Blanco tunnel closure chemistry. Report to Golcorp Cerro Blanco Geomega Inc.

Gzyl G, Banks D (2007) Verification of the "first flush" phenomenon in mine water from coal mines in the Upper Silesian Coal Basin. Poland J Cont Hydrol 92(1–2):66–86

Kesimal A, Yilmaz E, Ercikdi B (2004) Evaluation of paste backfill mixtures consisting of sulphide-rich mill tailings and varying cement contents. Cement Concrete Res 34(10):1817–1822. https://doi.org/10.1016/j.cemconres.2004.01.018

Langmuir D (1997) Aqueous environmental geochemistry. Prentice Hall

Langmuir D, Whittemore DO (1971) Variations in the stability of precipitated ferric oxyhydroxides. In: Hem JD (ed) Non-equilibrium systems in natural water chemistry. American Chemical Soc Symp Series 106

Leckie JO, Benjamin MM, Hayes KF, Kaufmann G, Altmann S (1980) Adsorption/coprecipitation of trace elements from water with iron oxyhydroxide (EPRI CS-1513). Stanford Univ Palo Alto CA. https://doi.org/10.2172/5101674

Maest AS, Kuipers JR, Travers CL, Atkins DA (2005) Predicting water quality at hardrock mines: methods and models, uncertainties, and state-of-the-art. Kuipers and Associates

MEND (1995) MINEWALL 2.0: user's manual. MEND Report 1.15.2a MEND Program

MEND (2006) Paste backfill geochemistry environmental effects of leaching and weathering (MEND Report). Mine Environment Neutral Drainage (MEND) Program

NDEP (Nevada Dept. of Environmental Protection) (2015) Nevada modified Sobek procedure summary 2015 Update. Bureau of Mining Regulation and Reclamation

NDEP (2020) Permanent closure of underground mine workings. Bureau of Mining Regulation and Reclamation BMRR NDEP

Newman CP, McCrea KW, Zimmerman J, Burke G, Andersen S (2019) Geochemistry, mineralogy, and acid-generating behaviour of efflorescent sulphate salts in underground mines in Nevada, USA. Geochem Expl Env Anal 19:317–329. https://doi.org/10.1144/geochem2018-074

Nordstrom DK (2017) Geochemical modeling and environmental systems. In: Nordstrom DK, Nicholson A (eds) Geochemical modeling for mine site characterization and remediation. SME, Littleton, pp 7–26

Nordstrom DK (2020) Geochemical modeling of iron and aluminum precipitation during mixing and neutralization of acid mine drainage. Minerals 10(6):547–559. https://doi.org/10.3390/min10060547

Parkhurst DL, Appelo CAJ (1999) User's guide to PHREEQC (Version 2): a computer program for speciation, batch-reaction, one-dimensional transport, and inverse geochemical calculations . Geol Water-Resourc Invest Rept 1:99–259. https://doi.org/10.3133/wri994259

Roesler AJ, Gammons CH, Druschel GK, Oduro H, Poulson SR (2007) Geochemistry of flooded underground mine workings influenced by bacterial sulfate reduction. Aquat Geochem 13:211–235

Schwertmann U, Taylor RM (1977) Iron oxides. In: Dixon JB, Weed SB (eds) Minerals in soil environments. Soil Science Soc of America, Madison, WI

SRK (2017) Deep south expansion project – cumulative effects, groundwater flow modeling report, crescent valley. Report to Barrick Cortez Inc, SRK Consulting (US) Inc

Tomiyama S, Igarashi T, Tabelin CB, Tangviroon P, Li H (2019) Acid mine drainage sources and hydrogeochemistry at the Yatani mine, Yamagata, Japan: a geochemical and isotopic study. J Contam Hydrol 225:103502. https://doi.org/10.1016/j.jconhyd.2019.103502

USGS (2015) Summary and Conclusions from The investigation of the effects of historical mining in the Animas River watershed, San Juan County, Colorado. In: Church SE, Guerard P, Finger SE (eds) Integrated investigations of environmental effects of historical mining in the animas river watershed. Geological Survey (USGS) Professional Paper

Younger PL (2000) Predicting temporal changes in total iron concentrations in groundwaters flowing from abandoned deep mines: a first approximation. J Contam Hydrol 44:47–69. https://doi.org/10.1016/S0169-7722(00)00090-5

Younger PL (2016) A simple, low-cost approach to predicting the hydrogeological consequences of coalfield closure as a basis for best practice in long-term management. Int J Coal Geol 164:25–34. https://doi.org/10.1016/j.coal.2016.06.002

Younger PL, Banwart SA, Hedin RS (2002) Mine water: hydrology, pollution. Kluwer Academic Publishers